remote sensing

MDPI

Article

A Novel Vital-Sign Sensing Algorithm for Multiple Subjects Based on 24-GHz FMCW Doppler Radar

Hyunjae Lee, Byung-Hyun Kim, Jin-Kwan Park and Jong-Gwan Yook *

Electrical and Electronic Engineering, Yonsei University, Seoul 120-749, Korea; dblovewls@yonsei.ac.kr (H.L.); bhkim159@hanmail.net (B.-H.K.); paladin91@yonsei.ac.kr (J.-K.P.)

* Correspondence: jgyook@yonsei.ac.kr

Received: 12 April 2019; Accepted: 17 May 2019; Published: 24 May 2019

Abstract: A novel non-contact vital-sign sensing algorithm for use in cases of multiple subjects is proposed. The approach uses a 24 GHz frequency-modulated continuous-wave Doppler radar with the parametric spectral estimation method. Doppler processing and spectral estimation are concurrently implemented to detect vital signs from more than one subject, revealing excellent results. The parametric spectral estimation method is utilized to clearly identify multiple targets, making it possible to distinguish multiple targets located less than 40 cm apart, which is beyond the limit of the theoretical range resolution. Fourier transformation is used to extract phase information, and the result is combined with the spectral estimation result. To eliminate mutual interference, the range integration is performed when combining the range and phase information. By considering breathing and heartbeat periodicity, the proposed algorithm can accurately extract vital signs in real time by applying an auto-regressive algorithm. The capability of a contactless and unobtrusive vital sign measurement with a millimeter wave radar system has innumerable applications, such as remote patient monitoring, emergency surveillance, and personal health care.

Keywords: vital sign monitoring; multiple subjects; parametric spectral estimation; mutual interference

1. Introduction

Heart rate and respiration are two essential vital signs that indicate the basic functioning of a human body [1–3]. They can be used for the diagnosis and prevention of cardiopulmonary diseases such as sleep apnea and arrhythmia. From this perspective, various researchers have contributed to the technical improvement of sensing methods for physiological signals, including heart rate and respiration. Among the various sensing methods for vital signs, non-contact and non-constraint sensors based on radio frequency (RF) and microwave techniques are promising approaches [4–7]. Non-contact vital sign sensors have the distinct advantage of possible continuous monitoring without patient perception; hence, they can be used for monitoring patients at risk of sudden infant death syndrome (SIDS) or sleep apnea [8,9]. In addition, they can be used as a home care service for the elderly through continuous monitoring system [10,11]. Furthermore, they can be used for a driver monitoring system for detecting and alerting drowsy driver [12–15].

However, in practical applications, non-contact RF vital sign sensors face a critical difficulty in detecting multiple subjects, which presents an inevitable problem for realistic applications. It is difficult to distinguish each vital sign, if there are two or more subjects within the radar beamwidth [16–20]. Recently, researchers have separated vital signs by using methods such as independent component analysis (ICA) or variational mode decomposition (VMD) [21,22]. However, because these methods merely separate signals, it is difficult to identify the subject of each vital sign. Thus, other techniques for extracting vital signs from multiple subjects must be developed. The strategy is to position subjects and extract vital signals at each location. The typical approaches are UWB radar [23–25]

and frequency-modulated continuous-wave (FMCW) Doppler radar. UWB radar has a high range resolution because of the wide bandwidth available through the emission of a narrow impulse; thus, it can easily localize the target. However, it is inefficient in terms of complexity and cost for the use of vital sign detection.

FMCW Doppler radar can extract both distance and phase information; thus, researchers have been interested in distinguishing the position of each subject and tracking vital signs. Recently, a hybrid radar system integrating FMCW mode and interferometry mode was developed [26–29]. Two-dimensional location is determined by FMCW radar incorporated with a mechanically or electronically rotating system and the vital sign is detected by an interferometry system based on CW radar. However, they excluded the situation where multiple subjects are within a beamwidth, especially for two adjacent subjects.

When there are two or more subjects within a beamwidth, it is not simple to distinguish each subject. Two major problems are target identification and mutual interference. Because a rear subject is relatively weaker than a front subject due to the path loss, a rear subject can be obscured by the signal of a front subject. In addition, when two subjects are close within the radar resolution limit caused by finite bandwidth, they can be overlapped. Moreover, even if they are separated, it is difficult to accurately detect each vital sign because of mutual interference. Therefore, clear target identification and mutual interference elimination are significant factors for vital sign monitoring of multiple subjects.

The present study proposes a novel vital-sign sensing algorithm for clear target identification and accurate vital sign estimation using a single 24 GHz FMCW Doppler radar based on FCC regulation. The proposed algorithm approaches the problem from three perspectives: (1) clear target identification; (2) elimination of mutual interference, especially in the case of two adjacent subjects within range resolution limit; and (3) vital sign retrieval with minimal ambient noise. For this purpose, with the proposed method, phase information is formed by the fast Fourier transform (FFT) method, while range information is obtained by the parametric spectral estimation method, which provides accurate and high-resolution results [30,31]. The physiological signals are extracted from the combined two types of information. The mutual interference is eliminated by range integration. Furthermore, each periodic vital signal is retrieved by the auto-regressive (AR) method [32,33]. For the performance validation of the proposed method, commercial piezoelectric sensors for breathing and heartbeat are used.

The remainder of this paper is structured as follows. In Section 2, the mechanism of the proposed algorithm is presented. In Section 3, simulation and experimental results of the proposed algorithm are demonstrated in various practical scenarios and the overall performance is verified.

2. Methods

2.1. Algorithm Architecture

Figure 1 shows a flow chart of the proposed vital sign-sensing algorithm for a plurality of targets. It consists of three steps: data acquisition, feature extraction, and vital sign detection. In the data acquisition step, the beat signal is obtained from the FMCW radar system. This signal is generated by deramp processing, which mixes the transmitted and received signals via a mixer and applies a low-pass filter to the mixer output. Range and phase information are concurrently extracted in the following step (i.e., feature extraction). The role of range estimation is to determine the number of subjects and provide distance information. The role of phase information is to determine the phase deviation caused by the Doppler effect at each location. This concurrent processing can provide more complete target information that cannot be obtained using Doppler processing alone. In the vital sign detection stage, vital sign information is extracted from phase data at each location acquired in feature extraction stage. Prior to extracting vital signs, the errors caused by dispersed human subjects are compensated by the range integration of the signals. Furthermore, the range integration reduces

mutual interference, performing an obvious signal separation even in a situation where two subjects are adjacent within the radar resolution limit. The AR method, which is a parametric estimation method, retrieves the vital sign data after integration. The details of each step are elaborated in the sections that follow.

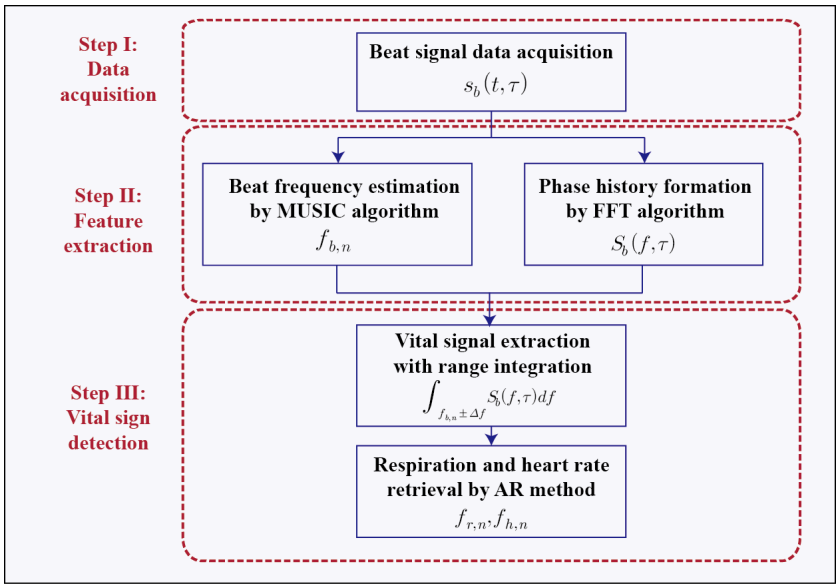

Figure 1. Flow chart of the proposed algorithm: (**I**) data acquisition from the radar system; (**II**) feature extraction for range and phase information in parallel; and (**III**) tracking vital signs.

2.2. Feature Extraction

In this step, the distance of each subject and the phase information necessary for the extraction of vital signs are simultaneously obtained by respective suitable methods. For multiple subjects, the time series beat signal at the kth modulation period is expressed as follows:

$$S_b(t,\tau) = \sum_{n=1}^{N} \rho_n \exp\left[j\left(2\pi\frac{2mR_n(\tau)}{c}t + \frac{4\pi f_c R_n(\tau)}{c}\right)\right], \quad t \in [(k-1)T_m,\ kT_m) \tag{1}$$

where N is the number of the target; t is the so-called "fast time"; τ is the so-called "slow time"; ρ_n is the reflectivity of the nth target, which is a function of the radar cross section (RCS) and range; m is the frequency modulation slope; R_n is the range of the nth target; f_c is the carrier frequency; and T_m is the modulation period. Physiological signals, such as respiration and heartbeat, are a very slow-moving target compared to the modulation frequency, making it appear as if the target is stationary during each modulation period. In other words, the target range is assumed to be constant for each period of frequency modulation by the stop-and-go hypothesis. Equation (1) consists of the sum of exponential functions with constant beat frequencies $f_{b,n} = 2mR_n/c$.

The phase information matrix can be formulated as follows using the Fourier transform:

$$S_b(f,\tau) = \sum_{n=1}^{N} \rho_n T_m \exp\left[j\frac{4\pi f_c R_n(\tau)}{c}\right] \mathrm{sinc}\left[T_m\left(f - f_{b,n}\right)\right]. \tag{2}$$

Equation (2) shows that, when there are two or more people in front of a radar, the accurate extraction of the beat frequency for each subject in the frequency domain is not straight forward, except for the most front target, due to the mutual interference between the reflected signals. Even further, if targets are placed within the theoretical resolution limit, the conventional FFT-based method cannot resolve multiple subjects because of the overlapped main lobes of the sinc functions. To overcome this problem, the MUSIC algorithm is utilized to provide accurate, precise, and high-resolution results in estimating the

beat frequency representing the range information. However, the MUSIC algorithm does not provide the necessary phase information; hence, the conventional FFT method is performed in conjunction with the MUSIC algorithm to provide phase information for each subject. Thus, the beat frequencies $f_{b,n}$ are obtained by the MUSIC algorithm, and the phase information matrix $S_b(f,\tau)$ is simultaneously generated by the FFT method at each modulation period. The detailed derivations of the formula for obtaining beat frequencies by the MUSIC algorithm are presented in the Supplementary Materials.

2.3. Vital Sign Detection

The range and phase information acquired in the preceding step are combined to retrieve vital signals for multiple subjects. The phase information is extracted from the FFT data, whose frequency is fixed at the beat frequency acquired by the MUSIC algorithm. The vital signal of the pth target can then be expressed as follows:

$$\begin{aligned} x_p(\tau) &= S_b(f_{b,p},\tau) \\ &= \rho_p T_m \exp\left[j\frac{4\pi f_c R_p(\tau)}{c}\right] + \sum_{\substack{n=1 \\ n\neq p}}^{N} \rho_n T_m \exp\left[j\frac{4\pi f_c R_n(\tau)}{c}\right] \operatorname{sinc}\left[T_m\left(f_{b,p}-f_{b,n}\right)\right]. \end{aligned} \tag{3}$$

In Equation (3), the first term shows the body movement of the pth target, while the second term describes the mutual interference from other subjects. The second term is a function of the sinc function; thus, its influence increases if two subjects approach each other, especially for the situation within the resolution limit. To reduce the effect of mutual interference, the integration of several cm is performed in consideration of the property of the sinc function.

For the ease of calculation, it is assumed that the total number of subjects is two and the RCSs of two subjects are identical. Because the human body is an electromagnetically dispersed target, the reflectivity ρ is proportional to $1/R$. Equation (2) can be expressed as follows:

$$S_b(f,\tau) = \alpha_1(f)\, y_1(\tau) + \alpha_2(f)\, y_2(\tau) \tag{4}$$

where

$$\begin{aligned} \alpha_1(f) &= \frac{\operatorname{sinc}\left[T_m\left(f-f_{b,1}\right)\right]}{R_1}, \quad \alpha_2(f) = \frac{\operatorname{sinc}\left[T_m\left(f-f_{b,2}\right)\right]}{R_2}, \\ y_1(\tau) &= \exp\left[j\frac{4\pi f_c R_1(\tau)}{c}\right], \quad y_2(\tau) = \exp\left[j\frac{4\pi f_c R_2(\tau)}{c}\right]. \end{aligned} \tag{5}$$

The effect of mutual interference depends on the ratio of coefficients α_1 and α_2 at each position. Thus, the mutual interference to signal ratio is α_2/α_1 at the position of R_1 and α_1/α_2 at the position of R_2. As the two subjects approach each other, the mutual interference increases, and each ratio of the coefficients also increases accordingly. Especially in the case of two adjacent subjects within the resolution limit, the vital sign is erroneously detected due to the mutual interference. Therefore, the ratio of coefficients should be reduced to detect the vital signs properly.

With the range integration, the vital signals of each subject can be formulated as follows:

$$\begin{cases} I_1(\tau) = \int_{f_{b,1}-\Delta f}^{f_{b,1}} S_b(f,\tau)\, df = y_1(\tau)y_{11} + y_2(\tau)y_{12} \\ I_2(\tau) = \int_{f_{b,2}}^{f_{b,2}+\Delta f} S_b(f,\tau)\, df = y_1(\tau)y_{21} + y_2(\tau)y_{22} \end{cases} \tag{6}$$

where

$$y_{11} = \int_{f_{b,1}-\Delta f}^{f_{b,1}} \alpha_1(f)df, \quad y_{12} = \int_{f_{b,1}-\Delta f}^{f_{b,1}} \alpha_2(f)df,$$
$$y_{21} = \int_{f_{b,2}}^{f_{b,2}+\Delta f} \alpha_1(f)df, \quad y_{22} = \int_{f_{b,2}}^{f_{b,2}+\Delta f} \alpha_2(f)df. \tag{7}$$

Thus, the mutual interference to signal ratio is y_{12}/y_{11} at the position of R_1 and y_{21}/y_{22} at the position of R_2. Figure 2 shows the mutual interference to signal ratio on each subject with varying the range difference. Despite the occurrence of some position estimation error, the vital signal of the front subject is robust to the mutual interference because of its relatively larger amplitude. On the other hand, the vital sign of the rear subject is susceptible to mutual interference. Thus, it is necessary to consider a method for removing the effect of mutual interference to the rear subject.

Assuming that the vital signs are correctly detected regardless of the mutual interference in a situation where range difference is larger than the resolution limit of 60 cm, the threshold value can be determined to be 0.45. The influence of the mutual interference is investigated based on the threshold value, as shown in Figure 3. When the error of the position estimation is −10 cm, a wider coverage area eliminates more mutual interference. However, when the error of the position estimation is 10 cm, a wider coverage area deteriorates the situation. According to the threshold value of the ratio, it is optimal to set the integration area to approximately 30 cm. When the integration area of 30 cm is applied, the mutual interference to signal ratio is less than the threshold value even in situation where the range difference is 40 cm, which can be called detection limit. On the other hand, the detection limit without range integration is 60 cm. This shows that the range integration is effective to eliminate the mutual interference for two adjacent subjects.

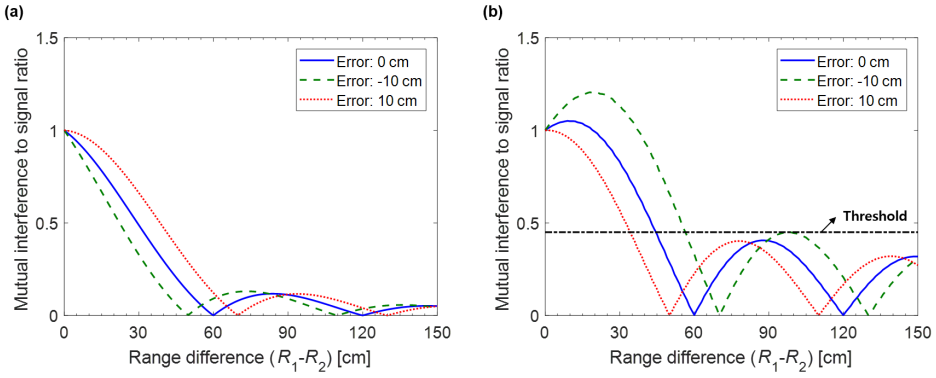

Figure 2. Influence of the mutual interference with varying range difference and position estimation error: (**a**) front subject (y_{12}/y_{11}); and (**b**) rear subject (y_{21}/y_{22}).

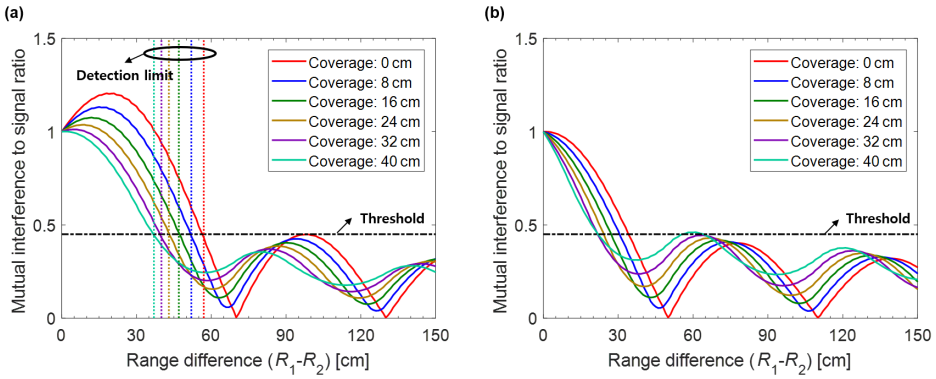

Figure 3. Effect of the range integration for the rear subject (y_{21}/y_{22}): (**a**) position estimation error: −10 cm; and (**b**) position estimation error: 10 cm.

Furthermore, some errors may arise in the data extracted from only one point, where the local maximum is displayed in the result of the MUSIC algorithm, because the human body is an electromagnetically disperse target. Therefore, the range integration not only corrects the errors in tracking vital signs, but also isolates vital signs from each other due to the characteristics of the sinc function, especially for adjacent subjects within the radar resolution limit.

Before the vital sign detection, the phase information is extracted from the output of the range integration at each position. Using the characteristics of the complex value, the arctangent demodulation is used for the extraction of the phase information. The extracted phase information of the pth target can be formulated as follows:

$$v_p(\tau) = \tan^{-1}\left[\frac{\Im\{I_p(\tau)\}}{\Re\{I_p(\tau)\}}\right]. \quad (8)$$

Detecting vital signs using the FFT method is difficult because Doppler radar systems are vulnerable to small-motion artifacts and ambient noise. Thus, the AR method, which has advantages in conditions where the objective to be interpreted is distinctly defined, is utilized to exploit the fact that pulse and breathing have a well-defined periodicity in viewpoint of the observation time of a few seconds. The detailed derivations of the formula for obtaining vital signs by the AR algorithm are presented in the Supplementary Materials.

3. Results and Discussion

3.1. Simulation Results

Simulations were conducted with the conventional FFT method and the proposed feature extraction method for two separation distances between two targets to evaluate the performance of the proposed algorithm for the vital sign detection of multiple targets: one closer than the theoretical range resolution and the other greater. No external noise or clutter was assumed to exist, but path loss was considered. Figure 4 shows the configuration of the simulation. The frequency range of the FMCW radar was from 24.00 to 24.25 GHz (i.e., it had a 250 MHz bandwidth, a resulting resolution limit of 60 cm, and a modulation frequency of 100 Hz). The displacements of the subject caused by respiration and heartbeat were assumed to be 10 and 0.3 mm, respectively. The respiration and the heart rate of the front target were 18 beats per minute (bpm) and 66 bpm, respectively, while those of the back target were 24 and 84 bpm, respectively.

Figure 4. Simulation setup.

In the first case, two subjects were placed at 120 cm and 300 cm from the radar, meaning that their separation distance was greater than the theoretical range resolution. Figure 5a shows the range estimation results. With the FFT method, a strong peak at the front subject position was clearly observed, but several peaks thereafter, causing range ambiguity for the rear target. The signal amplitude from the rear subject was considerably weaker than that of the front one; hence, the signal from the target behind was masked by the sidelobe of the front subject's signal. In contrast, when the proposed feature extraction method was applied, two subjects were clearly distinguished, as shown in Figure 5a. In the second case, two subjects were placed closer together than the theoretical range: one was at 120 cm, and the other was at 170 cm. As shown in Figure 5c, with the FFT method, two sinc

functions from the reflected signals of both subjects overlapped to form one peak. On the contrary, the proposed feature extraction method could distinctly detect the closely spaced subjects.

Phase information was utilized at the range of each subject, which was estimated by the proposed feature extraction method, to extract vital signs from each subject independently. The signal amplitude of the pulse signal was relatively smaller than that of the respiration signal; thus, detecting the heart rate signal was quite challenging. The normal frequency ranges of breathing and heartbeat signals are well defined. Both signals can be separately detected by appropriate bandpass filters. For typical adults, the resting heart rate is in the range between 60 and 100 bpm. Thus, the frequency range of the bandpass filter for respiration detection was delimited to between 0.2 and 0.8 Hz (i.e., 12–48 bpm), while that of the bandpass filter for heartbeat detection was 0.8–3 Hz (i.e., 48–180 bpm). Figure 5b,d shows the vital signs of each subject extracted from the AR method, revealing an excellent agreement.

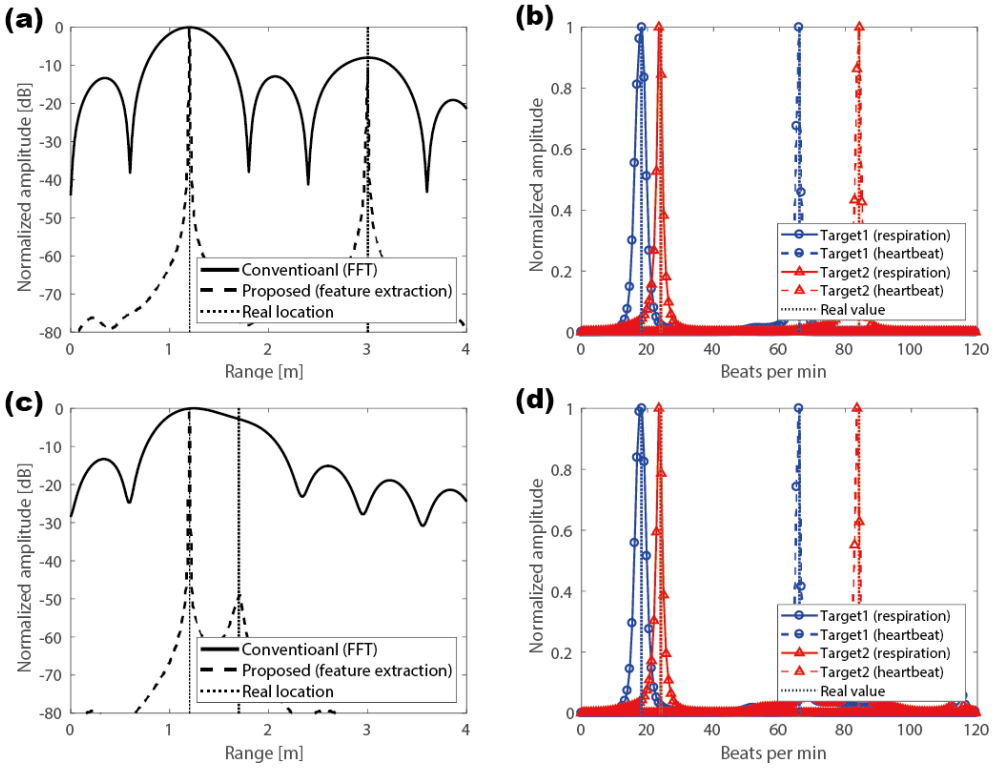

Figure 5. Simulation results for two targets: (**a**) range estimation for two targets at distances of 120 and 300 cm; (**b**) heart rate and respiration extraction for two targets at distances of 120 and 300 cm using the AR method; (**c**) range estimation for two targets at distances of 120 and 170 cm; and (**d**) heart rate and respiration extraction for two targets at distances of 120 and 170 cm using the AR method.

The third case was a more extreme case: two subjects were placed at 120 cm and 160 cm from the radar. Even in this extreme case, the proposed feature extraction method could clearly distinguish two subjects, as shown in Figure 6a. However, when the phase information was extracted at a single point, the vital signal detection was not performed normally. The mutual interference depicted in the second term of Equation (3) significantly increased; hence, the signal detection of front subject was impeded by the signal from the rear subject and the signal detection of rear subject was impeded by the signal from the front subject, as shown in Figure 6b. In contrast, with the range integration, the respective vital signs were accurately retrieved, as shown in Figure 6c.

In addition, to confirm the effectiveness of the proposed method in noisy environments, the root mean square error (RMSE) was calculated as a function of signal-to-noise ratio (SNR) for the following two examples: (1) two subjects located at 120 cm and 300 cm; and (2) two subjects located at 120 cm and 160 cm. The range was estimated by the proposed feature extraction method and the vital sign

was detected by AR method. When two subjects were placed farther than the theoretical resolution limit, they were clearly identified and each vital sign was accurately detected, as shown in Figure 7a–c. Because the separation distance was large, the effect of mutual interference was negligible, thus the range integration hardly affected the detection accuracy. In Figure 7c, the range integration appeared to increase the error, but the difference was insignificant owing to the value below −35 dB. When two subjects were placed closer than the theoretical resolution limit, they were clearly identified over a SNR of 15 dB. Although the range was accurately detected, the heart rate of each target showed different results because of the mutual interference, as shown in Figure 7e,f. However, with the range integration, the vital signs were exactly detected. In summary, it was confirmed that, even if the targets were placed within the theoretical range resolution limit, the proposed algorithm can accurately extract the vital signs once the SNR exceeds 15 dB. This verifies that the proposed algorithm is suitable for vital sign detection of multiple subjects, especially in the case of two adjacent subjects within the resolution limit.

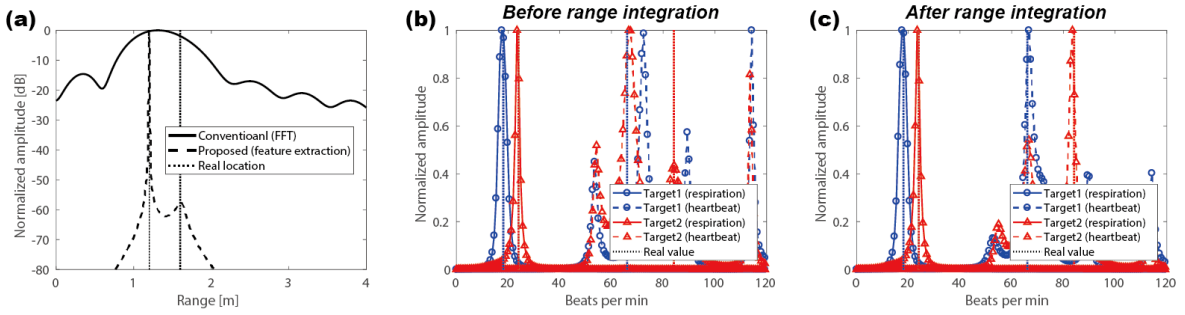

Figure 6. Simulation results for two subjects at distances of 120 and 160 cm: (**a**) range estimation; (**b**) vital sign detection without the range integration; and (**c**) vital sign detection with the range integration.

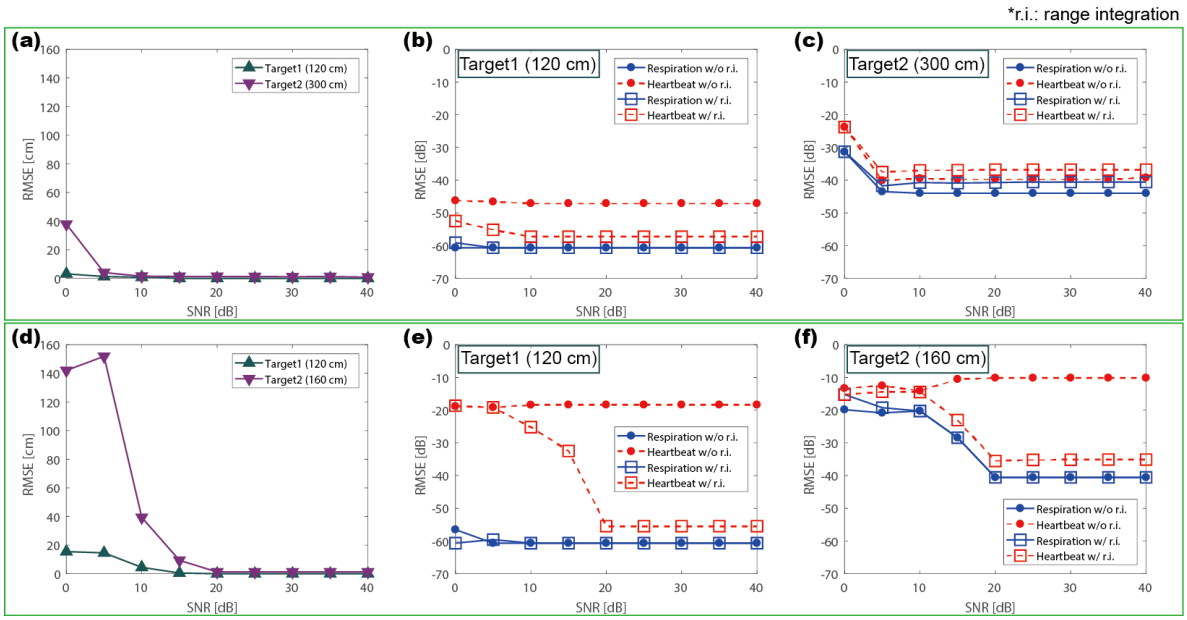

Figure 7. Root mean square error (RMSE) according to SNR for the proposed algorithm: (**a**) RMSE of range estimation at distances of 120 and 300 cm; (**b**) RMSE of heart rate and respiration detection for the front target at a distance of 120 cm (rear target: 300 cm); (**c**) RMSE of heart rate and respiration detection for the rear target at a distance of 300 cm (front target: 120 cm); (**d**) RMSE of range estimation at distances of 120 and 160 cm; (**e**) RMSE of heart rate and respiration detection for the front target at a distance of 120 cm (rear target: 160 cm); and (**f**) RMSE of heart rate and respiration detection for the rear target at a distance of 160 cm (front target: 120 cm).

3.2. Measurement Procedure

Piezoelectric transducer sensors for breathing (UFI-1132, UFI) and heartbeat (UFI-1010, UFI) were used for comparison to validate the performance of the proposed algorithm. The bandwidth of the FMCW Doppler radar (IVS-162, InnoSenT) was 250 MHz, which is compliant with FCC regulations (i.e., from 24.00 to 24.25 GHz). The equivalent isotropic radiated power (EIRP) is 15 dBm. The horizontal 3 dB beamwidth is 45° and the vertical 3 dB beamwidth is 38°. The horizontal sidelobe suppression is 15 dB and the vertical sidelobe suppression is 20 dB. The real-time signal was digitized by the data acquisition board (DAQ: NI-9234) and saved by a custom LabVIEW setup. The modulation frequency was 100 Hz, and the sampling rate was 6400 samples/s.

The experiments were conducted in a fixed state with sitting chairs. When performing measurements for the vital signs of two people, subjects were positioned within the beam width of the radar. In performance verification, only the line-of-sight (LOS) situation for each subject was considered without regard to the azimuth angle. Figure 8 presents the experimental setup for two people.

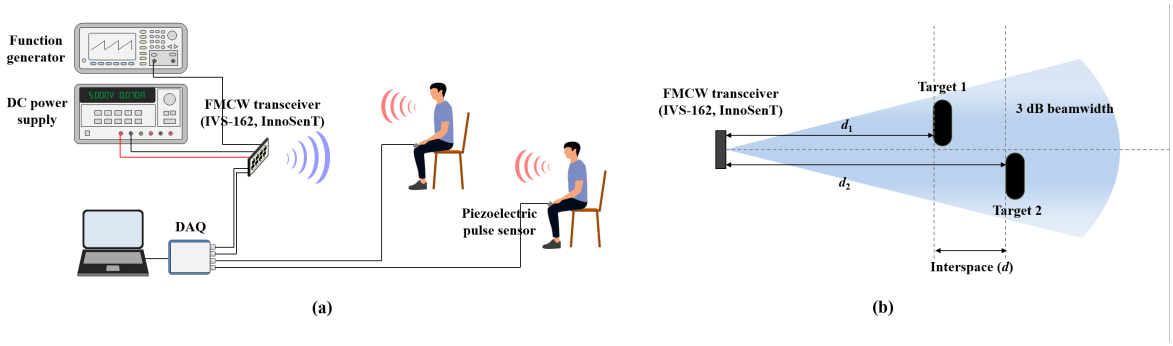

Figure 8. Experimental setup: (**a**) overview; and (**b**) top view.

3.3. Measurement Results

Two different experiments were conducted to validate the performance of the proposed algorithm: (1) a single-subject measurement as a function of the distance from the radar; and (2) multiple-subject measurement as a function of the separation distance between the two subjects. The measurements were taken in an indoor hallway, and the target range decided was the distance from the radar to the human subject.

3.3.1. Single-Subject Measurement

The single-subject measurement was performed to confirm the stability and the reliability of the proposed algorithm. The target range was set at intervals of 60 cm from 120 to 300 cm. Figure 9a,b represents the measurement results at a distance of 300 cm. The resolution of the target range appeared to be relatively large compared to that in the simulation results because of the ambient noise and disperse human body targets. Nevertheless, the estimated locations, where the maximum value of the results were observed, were in good agreement with the actual distance. As a result of extracting phase information at the estimated location, the heartbeats and the respiration signals obtained via an appropriate bandpass filter agreed very well with the signals obtained from the piezoelectric sensor. Figure 9c summarizes multiple measurement results as a function of the distance from the radar to the subject, revealing an excellent agreement with errors of less than 10 cm.

3.3.2. Multiple-Subject Measurement

Multiple-subject measurements were conducted in two different scenarios based on distance: (i) where the interval between the two targets is greater than the theoretical range resolution; and (ii) where the interval is smaller than the theoretical range resolution.

First, the two subjects were positioned at 130 and 300 cm away from the radar such that the distance between the subjects was larger than the theoretical range resolution of 60 cm. Figure 10a represents the normalized amplitude of the received signal in the distance domain. The amplitude of the front target was relatively larger than that of the rear target. As a result, the signal information obtained by the FFT method did not distinguish the signal from the rear target because it was masked by the sidelobe of the sinc function. On the other hand, the results obtained using the proposed method clearly displayed the location of the subject signal despite the large signal difference between the front and rear targets. For real-time data, the short-time autoregressive (STAR) method was performed at 1 s intervals with 10 s windows. The detailed derivations of STAR are presented in the Supplementary Materials. Figure 10b,c shows the real-time vital signals extracted at each subject position with the proposed method. Figure 10d shows the extracted peak values of the real-time data for each sensor, and Figure 10e shows the spectrum analysis result of total time data for each sensor. The results agreed well with the reference finger sensor data in both cases, as shown in Figure 10d,e.

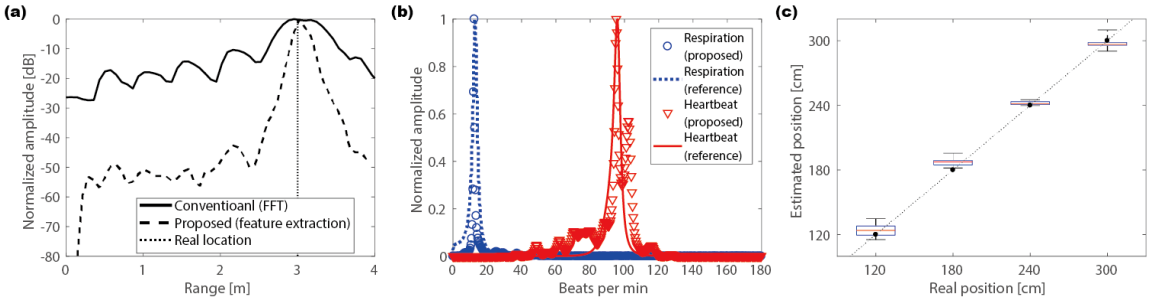

Figure 9. Measurement results for a single person at a distance of 300 cm: (**a**) range estimation; (**b**) heart rate and respiration; and (**c**) range estimation varying with distance from the radar.

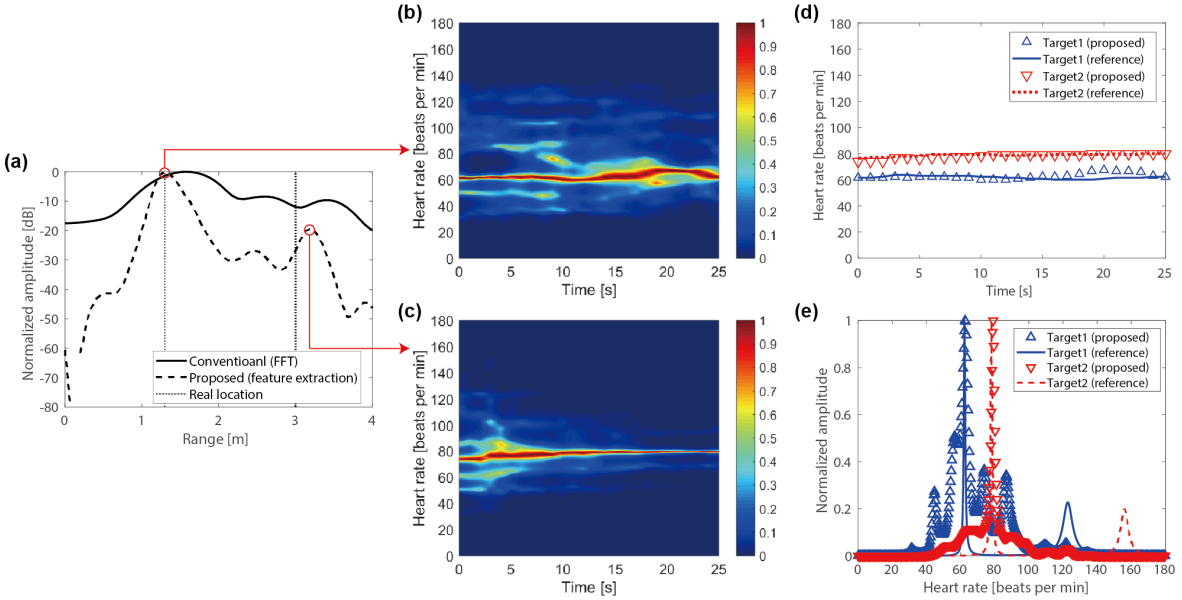

Figure 10. Measurement results for two targets: (**a**) range estimation for two targets at distances of 130 to 300 cm; (**b**) real-time heart rate for the front target at a distance of 130 cm; (**c**) real-time heart rate for the rear target at a distance of 300 cm; (**d**) comparison between the proposed method and the reference sensor in real-time data; and (**e**) comparison between the proposed method and the reference sensor in terms of the total time.

Second, Figure 11a shows the measurement results in the case where two subjects were placed at 130 and 170 cm away from the radar, which was closer than the theoretical distance resolution. In the results acquired using the FFT method, distinguishing each subject was difficult because of

the overlapping signals from the two adjacent people. By contrast, the proposed method clearly distinguished the positions of the two people. Interestingly, despite the accurate localization, the vital sign of the rear subject did not coincide with the reference sensor data, as shown in Figure 11d,e. It provided the vital sign of the front subject, not the rear subject because of the large signal interference. With the range integration, the proposed method obviously compensated the mutual interference, revealing an excellent agreement with the reference sensor data, as shown in Figure 12.

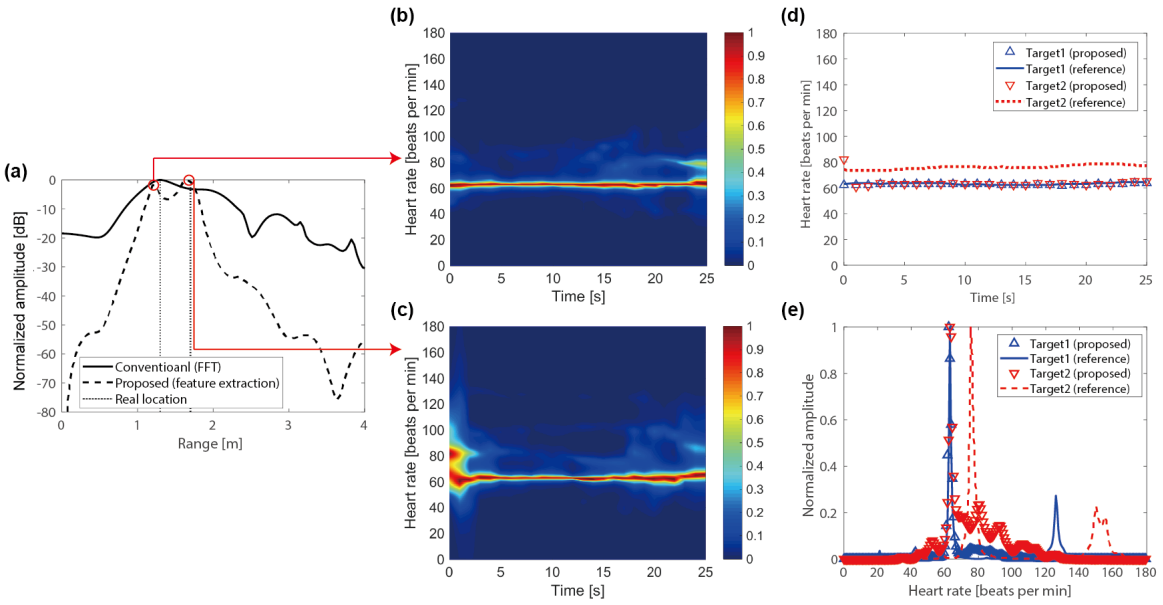

Figure 11. Measurement results for two targets: (**a**) range estimation for two targets at distances of 130 to 170 cm; (**b**) real-time heart rate for the front target at a distance of 130 cm; (**c**) real-time heart rate for the rear target at a distance of 170 cm; (**d**) comparison between the proposed method and the reference sensor in terms of the real-time data; and (**e**) comparison between the proposed method and the reference sensor in terms of the total time.

Additionally, the measurement for the three subjects was conducted. Figure 13a shows the measurement results in the case where the three subjects were placed at 130, 180 and 300 cm away from the radar. The FFT method did not distinguish the three subjects. On the other hand, the proposed method clearly distinguished the positions of the three people. Furthermore, despite some errors in the range estimation, the vital signs of each subject correctly coincide with the reference data, as shown in Figure 13b–e.

Lastly, the measurements were conducted 15 times each by varying the distance between the two subjects to evaluate the sensor reliability. The front person was fixed at a distance of 130 cm away from the radar. The distance to the rear person was changed from 170 to 300 cm (Table 1). The proposed sensor detected the heart rate to within an error of 5 bpm, regardless of the distance between the subjects. Furthermore, with the range integration, it provided precise results with the low standard deviation, especially in the case of the adjacent two subjects within the radar resolution limit. In Cases 1, 4 and 5, the accuracy of the rear subject appears to be better than that of the front subject. It is caused by the difference in the degree of the minute motion artifacts. However, considering that the 1% error in the heart rate of 60 bpm implies an error of 0.6 bpm, the difference between the detection accuracy of the front and rear subjects is negligible.

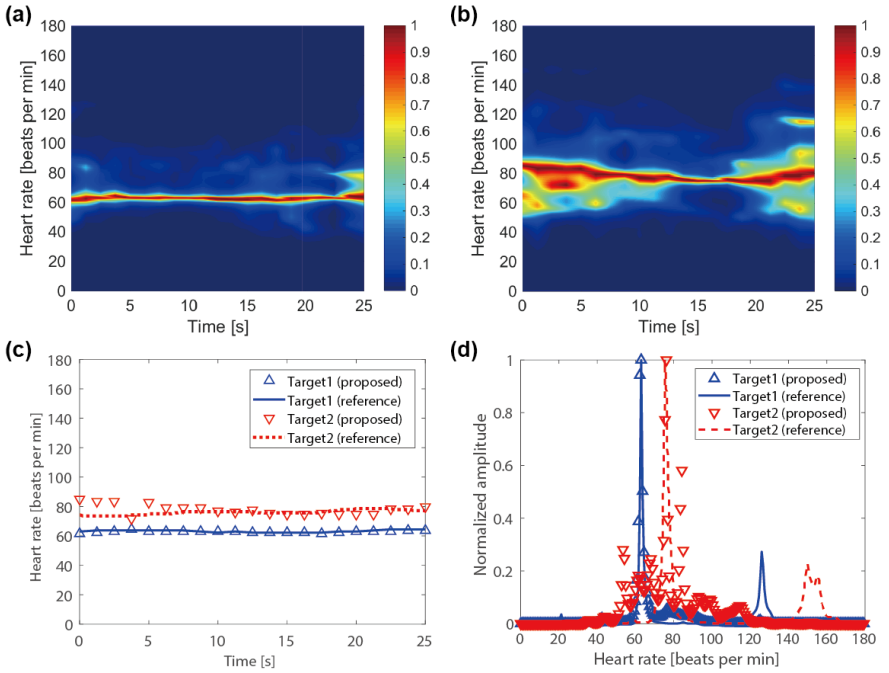

Figure 12. Compensated measurement results for two targets with the range integration: (**a**) real-time heart rate for the front target at a distance of 130 cm; (**b**) real-time heart rate for the rear target at a distance of 170 cm; (**c**) comparison between the proposed method and the reference sensor in terms of the real-time data; and (**d**) comparison between the proposed method and the reference sensor in terms of the total time.

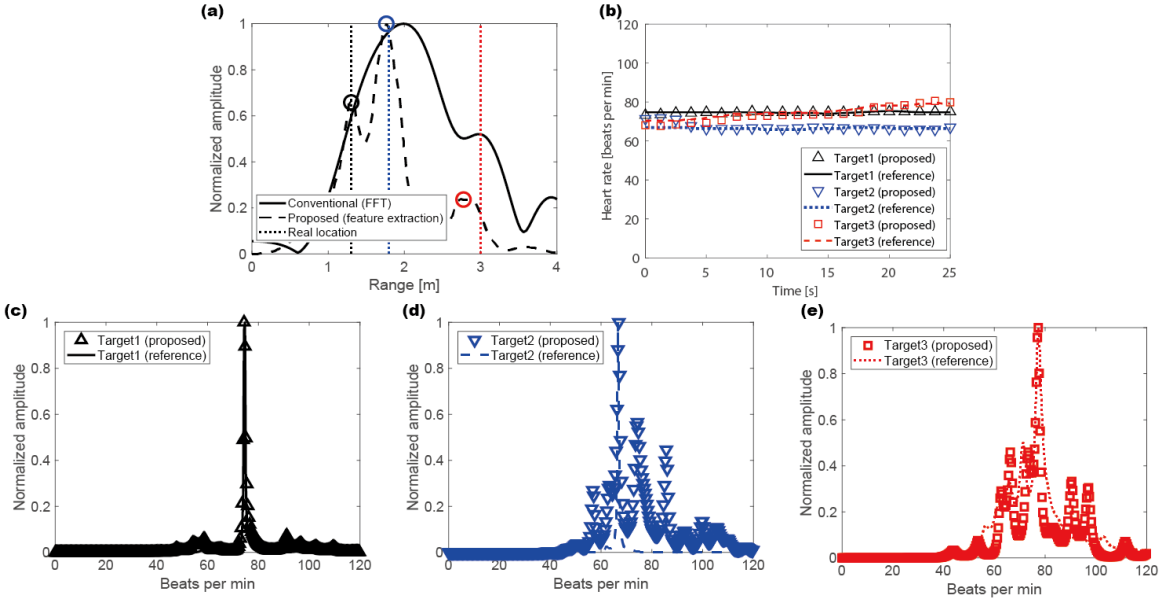

Figure 13. Measurement results for three targets: (**a**) range estimation for three targets at distances of 130, 180 and 300 cm; (**b**) comparison between the proposed method and the reference sensor in terms of the real-time data; (**c**) heart rate for target 1 in terms of total time; (**d**) heart rate for target 2 in terms of total time; and (**e**) heart rate for target 3 in terms of total time.

Table 1. Repeatability test of detection accuracy for vital signs.

Case	Subject	Location	Detection Accuracy	
			w/o Range Integration	**w/ Range Integration**
1	Front	130 cm	93.98% ± 6.99 %	96.99% ± 4.21%
	Rear	300 cm	91.72% ± 8.84%	97.24% ± 3.28%
2	Front	130 cm	99.12% ± 0.79%	99.22% ± 1.33%
	Rear	260 cm	93.29% ± 7.58%	96.28% ± 5.46%
3	Front	130 cm	96.46% ± 8.53%	98.32% ± 2.39%
	Rear	220 cm	94.28% ± 4.77%	94.47% ± 5.32%
4	Front	130 cm	92.74% ± 9.21%	97.13% ± 5.50%
	Rear	180 cm	88.39% ± 9.89%	97.20% ± 1.96%
5	Front	130 cm	98.62% ± 1.21%	98.88% ± 1.91%
	Rear	170 cm	84.02% ± 15.52%	99.27% ± 0.41%

3.4. Discussion

The proposed algorithm provided an outstanding performance. It is verified that the proposed method can detect the vital signs for two subjects in a direction using a single radar. When two subjects are closer than 40 cm, it is possible to identify the subjects by the proposed feature extraction method, but the vital signs are erroneously detected owing to the significant mutual interference. Therefore, the detection limit of the proposed method is 40 cm, which is superior to the theoretical resolution limit and has sufficient efficiency. Because the range used in this study is the distance between the radar and the chest of a human body, it is possible to distinguish between two subjects approximately 20–30 cm apart by considering the thickness of the human body. Furthermore, combining the proposed method with a beam-steering system, it is possible to detect the position and vital signs in a two-dimensional situation.

Although the results of the proposed method suggested excellent performance, there are a few issues to consider for practical application. One is the suppression of clutters. The MUSIC algorithm cannot separate the stationary clutter because it does not provide the phase information. It can be solved by the micro-Doppler effect. A stationary target and a moving target can be distinguished by the standard deviation of phase information. After target identification by the MUSIC algorithm, the stationary clutters can be separated by the micro-Doppler effect. Another is the motion artifact, which is an inevitable issue for the vital sign sensor. The signals of the subtle movements such as hand gestures or legs shaking are much larger than the vital signs, making it difficult to detect the vital sign while moving. The other is sidelobe suppression. When the sidelobe suppression is not sufficiently achieved, it makes the ghost image of the target located on the direction of the sidelobe. It degrades the performance of the proposed algorithm. To eliminate the performance degradation due to sidelobe effect, the sidelobe should be lowered enough when designing an antenna. Therefore, these issues need to be resolved for further real applications.

4. Conclusions

A novel remote non-contact vital-sign sensing algorithm for multiple subjects is proposed based on a 24 GHz FMCW Doppler radar using the parametric spectral estimation technique. This algorithm utilizes high-resolution signal processing techniques to overcome the ambiguity of range detection based on the conventional FFT method. Vital signs not only for one person, but also for a plurality of people can be retrieved in real time by integrating range detection with the high-resolution method and phase information extracted from the conventional FFT method. The proposed algorithm can detect the vital signs of two adjacent people less than 40 cm apart by overcoming the theoretical range resolution at the given frequency bandwidth. We envision that this approach can be applied to various practical situations, such as home care, medical assistance, and driver-monitoring systems.

Supplementary Materials: The following are available online at http://www.mdpi.com/2072-4292/11/10/1237/s1.

Author Contributions: H.L. developed most of the methodology and validated the results. B.-H.K. and J.-K.P. provided valuable suggestions on the research. J.-G.Y. supervised the project and provided valuable advice on conducting the work. All authors contributed to writing the final manuscript.

Funding: This research received no external funding.

Acknowledgments: This work was supported by the National Research Foundation of Korea (NRF) grant funded by the Korea government (MSIT) (NRF-2017R1A2B2011724).

Conflicts of Interest: The authors declare no conflict of interest.

References

1. Kwak, Y.H.; Kim, W.; Park, K.B.; Kim, K.; Seo, S. Flexible heartbeat sensor for wearable device. *Biosens. Bioelectron.* **2017**, *94*, 250–255. [CrossRef]
2. Shafiq, G.; Veluvolu, K.C. Surface chest motion decomposition for cardiovascular monitoring. *Sci. Rep.* **2014**, *4*, 5093. [CrossRef]
3. Will, C.; Shi, K.; Schellengberger, S.; Steigleder, T.; Michler, F.; Fuchs, J.; Weigel, R.; Ostgathe, C.; Koelpin, A. Radar-based heart sound detection. *Sci. Rep.* **2018**, *8*, 11551. [CrossRef]
4. Hong, Y.; Kim, S.G.; Kim, B.H.; Ha, S.J.; Lee, H.J.; Yun, G.H.; Yook, J.G. Noncontact proximity vital sign sensor based on pll for sensitivity enhancement. *IEEE Trans. Biomed. Circuits Syst.* **2014**, *8*, 584–593. [CrossRef] [PubMed]
5. Kim, B.H.; Hong, Y.; An, Y.J.; Kim, S.G.; Lee, H.J.; Kim, S.W.; Hong, S.B.; Yun, G.H.; Yook, J.G. A proximity coupling RF sensor for wrist pulse detection based on injection-locked PLL. *IEEE Trans. Microw. Theory Tech.* **2016**, *64*, 1667–1676. [CrossRef]
6. Suzuki, S.; Matsui, T.; Kawahara, H.; Ichiki, H.; Shimizu, J.; Kondo, Y.; Gotoh, S.; Yura, H.; Takase, B.; Ishihara, M. A non-contact vital sign monitoring system for ambulances using dual-frequency microwave radars. *Med. Biol. Eng. Comput.* **2009**, *47*, 101–105. [CrossRef] [PubMed]
7. Li, C.; Lin, J.; Xiao, Y. Robust overnight monitoring of human vital signs by a non-contact respiration and heartbeat detector. In Proceedings of the 2006 International Conference of the IEEE Engineering in Medicine and Biology Society, New York, NY, USA, 30 August–3 September 2006; pp. 2235–2238. [CrossRef]
8. Hong, H.; Zhang, L.; Gu, C.; Li, Y.; Zhou, G.; Zhu, X. Noncontact sleep stage estimation using a CW doppler radar. *IEEE J. Emerg. Sel. Top. Circuits Syst.* **2018**. [CrossRef]
9. Adib, F.; Mao, H.; Kabelac, Z.; Katabi, D.; Miller, R.C. Smart homes that monitor breathing and heart rate. In Proceedings of the 33rd Annual ACM Conference on Human Factors in Computing Systems (CHI'15), Seoul, Korea, 18–23 April 2015; pp. 837–846. [CrossRef]
10. Lin, F.; Zhuang, Y.; Song, C.; Wang, A.; Li, Y.; Gu, C.; Li, C.; Xu, W. Sleepsense: A noncontact and cost-effective sleep monitoring system. *IEEE Trans. Biomed. Circuits Syst.* **2017**, *11*, 189–202. [CrossRef]
11. Wang, J.; Li, C. A human tracking and physiological monitoring fsk technology for single senior at home care. In Proceedings of the 2018 40th Annual International Conference of the IEEE Engineering in Medicine and Biology Society (EMBC), Honolulu, HI, USA, 18–21 July 2018; pp. 4432–4435. [CrossRef]
12. Lee, K.J.; Park, C.; Lee, B. Tracking driver's heart rate by continuous-wave doppler radar. In Proceedings of the 2016 38th Annual International Conference of the IEEE Engineering in Medicine and Biology Society (EMBC), Orlando, FL, USA, 16–20 August 2016; pp. 5417–5420. [CrossRef]
13. Chen, L.; Yang, X.; Fu, P.; Xu, Z.; Zhang, C. Novel doppler approach to monitoring driver drowsiness. *Electron. Lett.* **2016**, *52*, 2011–2013. [CrossRef]
14. Park, J.K.; Hong, Y.; Lee, H.; Jang, C.; Yun, G.H.; Lee, H.J.; Yook, J.G. Noncontact RF Vital Sign Sensor for Continuous Monitoring of Driver Status. *IEEE Trans. Biomed. Circuits Syst.* **2019**. [CrossRef]
15. Mercuri, M.; Liu, Y.H.; Lorato, I.; Torfs, T.; Wieringa, F.; Bourdoux, A.; Van Hoof, C. A direct phase-tracking doppler radar using wavelet independent component analysis for non-contact respiratory and heart rate monitoring. *IEEE Trans. Biomed. Circuits Syst.* **2018**, *12*, 632–643. [CrossRef]
16. Boric-Lubecke, O.; Lubecke, V.M.; Host-Madsen, A.; Samardzija, D.; Cheung, K. Doppler radar sensing of multiple subjects in single and multiple antenna systems. In Proceedings of the TELSIKS 2005—2005 uth

International Conference on Telecommunication in ModernSatellite, Cable and Broadcasting Services, Nis, Serbia, 28–30 September 2005; Volume 1, pp. 7–11. [CrossRef]
17. Hu, W.; Zhao, Z.; Wang, Y.; Zhang, H.; Lin, F. Noncontact accurate measurement of cardiopulmonary activity using a compact quadrature doppler radar sensor. *IEEE Trans. Biomed. Eng.* **2014**, *61*, 725–735. [CrossRef]
18. Zhou, Q.; Liu, J.; Host-Madsen, A.; Boric-Lubecke, O.; Lubecke, V. Detection of multiple heartbeats using doppler radar. In Proceedings of the 2006 IEEE International Conference on Acoustics Speech and Signal Processing Proceedings, Toulouse, France, 14–19 May 2006; Volume 2. [CrossRef]
19. Li, C.; Lubecke, V.M.; Boric-Lubecke, O.; Lin, J. A review on recent advances in doppler radar sensors for noncontact healthcare monitoring. *IEEE Trans. Microw. Theory Tech.* **2013**, *61*, 2046–2060. [CrossRef]
20. Li, C.; Peng, Z.; Huang, T.Y.; Fan, T.; Wang, F.K.; Horng, T.S.; Munoz-Ferreras, J.M.; Gomez-Garcia, R.; Ran, L.; Lin, J. A review on recent progress of portalbe short-range noncontact microwave radar systems. *IEEE Trans. Microw. Theory Tech.* **2017**, *65*, 1692–1706. [CrossRef]
21. Yue, S.; He, H.; Wnag, H.; Rahul, H.; Katabi, D. Extracting multi-person respiration from entangled rf signals. *Proc. ACM Interact. Mob. Wearable Ubiquitous Technol.* **2017**, *2*, 86. [CrossRef]
22. Ding, C.; Yan, J.; Zhang, L.; Zhao, H.; Hong, H.; Zhu, X. Noncontact multiple targets vital sign detection based on vmd algorithm. In Proceedings of the 2017 IEEE Radar Conference (RadarConf), Seattle, WA, USA, 8–12 May 2017. [CrossRef]
23. Khan, F.; Cho, S.H. A detailed algorithm for vital sign monitoring of a stationary/non-stationary human through ir-uwb radar. *Sensors* **2017**, *17*, 290. [CrossRef]
24. Rivera, N.V.; Venkatesh, S.; Anderson, C.; Buehrer, R.M. Multi-target estimation of heart and respiration rates using ultra wideband sensors. In Proceedings of the 2006 14th European Signal Processing Conference, Florence, Italy, 4–8 September 2006; pp. 1–6.
25. Ren, L.; Koo, Y.S.; Wang, H.; Wang, Y.; Liu, Q.; Fathy, A.E. Noncontact multiple heartbeats detection and subject localization using uwb impulse doppler radar. *IEEE Microw. Wirel. Compon. Lett.* **2015**, *25*, 690–692. [CrossRef]
26. Wang, F.K.; Horng, T.S.; Peng, K.C.; Jau, J.K.; Li, J.Y.; Chen, C.C. Detection of concealed individuals based on their vital signs by using a see-through-wall imaging system with a self-injection-locked radar. *IEEE Trans. Microw. Theory Tech.* **2013**, *61*, 696–704. [CrossRef]
27. Wang, G.; Gu, C.; Inoue, T.; Li, C. A hybrid fmcw-interferometry radar for indoor precise positioning and versatile life activity monitoring. *IEEE Trans. Microw. Theory Tech.* **2014**, *62*, 2812–2822. [CrossRef]
28. Peng, Z.; Ran, L.; Li, C. A *k*-band portable fmcw radar with beamforming array for short-range localization and vital doppler targets discrimination. *IEEE Trans. Microw. Theory Tech.* **2017**, *65*, 3443–3452. [CrossRef]
29. Peng, Z.; Li, C. A portalbe *k*-band 3-d mimo radar with nonuniformly spaced array for short-range localization. *IEEE Trans. Micrw. Theory Tech.* **2018**, *66*, 5075–5086. [CrossRef]
30. Stoica, P.; Moses, R.L. *Spectral Analysis of Signals*; Pearson Prentice Hall: Upper Saddle River, NJ, USA, 2005.
31. Schmidt, R. Multiple emitter location and signal parameter estimation. *IEEE Trans. Antennas Propag.* **1986**, *34*, 276–280. [CrossRef]
32. Tarassenko, L.; Villarroel, M.; Guazzi, A.; Jorge, J; Clifton, D.; Pugh, C. Non-contact video-based vital sign monitoring using ambient light and auto-regressive models. *Physiol. Meas.* **2014**, *35*, 807. [CrossRef] [PubMed]
33. Kim, S.G.; Yun, G.H.; Yook, J.G. Wireless rf vital signal sensor using autoregressive spectral estimation method. *IEEE Antennas Wirel. Propag. Lett.* **2012**, *11*, 535–538. [CrossRef]